International Research Journal of Engineering and Technology (IRJET) e-ISSN: 2395-0056
Volume: 13 Issue: 06 | Jun 2026 www.irjet.net p-ISSN: 2395-0072

Modeling Surface Water Dynamics Using Coat Net and GIS-Based Spatial Analytics for Enhanced Hydrological Assessment

K N Rukmini Florence[1], D V Satyanarayana Moorthy[2], P Vikranth[3]

[1]Dept. of Civil Engineering, SVU College of Engineering, AP, India
[2]Professor, Dept. of Civil Engineering, SVU College of Engineering, AP, India
[3]Associate Technical Manager, Mavenir Systems Private Limited, Bangalore, Karnataka, India

---

Abstract - *Hydrological assessment is the analysis of water resources, centered on the flow, distribution, and accessibility of surface and groundwater within a watershed. This research conveys a detailed understanding of the hydrological behavior of the Pulicat lake using advanced modeling techniques. The slope and orientation of the lake are characterized by using a spatial analysis system and remote sensing techniques. The baseflow and surface runoff of the Sullurpeta and Dugarajupatnam watershed during 2001 to 2019 are simulated using recursive digital filter techniques. To reduce the uncertainty of the model, a sensitivity analysis is carried on the Soil and Water Assessment Tool (SWAT) key parameters. The p and t validations are significant for precipitation, temperature, and curve number, displaying low p-values and strong t-statistics. The error values of the calibration phase during 2001 to 2009 and validation phase during 2010 to 2019 are 0.22 and 0.31, respectively, illustrating the validity and strength of the SWAT model. The spatial analytics of Pulicat lake by a hybrid Convolution–Transformer Network (CoatNet) explored the east zone as the central node for connectivity and flow. The error in predicting global integration is relatively low, and global choice has the highest error of 17.95 %. On average, the model possesses a 15% error rate, which is considered acceptable in spatial and hydrological modeling, showing that the framework produces reliable results. Together, these methods provide a complete insight into the hydrological response of the research area, supporting reliable assessment and sustainable watershed management.*

Key Words: Hydrological Modeling, Pulicat Lake, Advanced Modeling Techniques, Parameter Estimation, Hybrid Network, Spatial Analytics, Watershed Management.

1. INTRODUCTION

Hydrological research studies the distribution, movement, and quality of water on the terrestrial surface and in the atmosphere [1]. It is vital for managing water resources, assessing environmental impacts from human activities, and ensuring water availability for both human and ecological systems [2]. Hydrological investigations are vital in many fields, comprising engineering, environmental sciences, and water resource management, although they have different goals, focus on various themes, and employ different methods [3,4]. In recent decades, hydrological modeling has become a central component of modern water resource management [5]. This development reflects the increasing pressure on global water systems caused by human activities and climate variability [6,7].

This research conveys a detailed understanding of the hydrological behavior of the Pulicat lake watershed by simulating baseflow and surface runoff using advanced modeling techniques. It aids in water resource planning, wetland conservation, and flood mitigation in a climate-sensitive coastal region. The outcomes support sustainable watershed management and policy formulation for the Pulicat lake ecosystem. The present research implemented two watersheds, as defined by the locations of two hydrological observation stations near the Sullurpeta watershed and Dugarajupatnam watershed, respectively. When combined with advanced deep learning architectures, the modeling of surface water dynamics is done accurately. Such integration is particularly valuable for climate-sensitive and ecologically fragile regions, where reliable hydrological assessments are crucial for water resource planning, wetland conservation, and flood management. By incorporating both time-series meteorological data and static watershed parameters, the research provides a comprehensive understanding of hydrological responses and supports sustainable watershed management and policy development.

A general overview of hydrological assessment is provided in section 1. Section 2 contains the literature review, and the proposed methodology is included in section 3. The results and discussion of the research are presented in section 4, where the hydrological behavior of the Pulicat lake is analyzed using advanced modeling techniques and a hybrid deep learning approach. Finally, section 5 offers the conclusion and the future scope of this research.

2. LITERATURE REVIEW

Wang et al., (2025) [8] provided essential sources for interpreting the nitrate source variation, controlling, and eliminating excess nitrate in the integrated water system in similar large freshwater areas. **Wang et al.,** (2025) [9] analyzed the dynamic contact angle consequence in dynamics of liquid–liquid absorption, was precisely described, clarifying the functional mechanism of osmotic pressure, and contributed theoretical justification for improving hydrocarbon extraction from shale reservoirs. **Lyu et al.,**

(2025) [10] provided an empirical framework for evaluating aquifer restoration outcomes on groundwater and surface and groundwater interactions, providing an adaptable approach for similar hydrogeological conditions. **Bojer et al.,** (2025) [11] underscored the significance of climatic elements in coordinating stream discharge and the need for sustainable land management to restrict negative environmental effects on water resources. **Shiferaw et al.,** (2025) [12] contributed to an advanced knowledge of interrelated processes between society and the environment, reinforcing and integrating nature-based approaches for sustainable and balanced land use. **Liu et al.,** (2025) [13] illustrated anthropogenic drought, the integrated two-system approach, which formalizes pathways and socio-hydrological interactions. The dual system provides an extensively relevant method for investigating man-made drought occurrences. **Kumar et al.,** (2025) [14] underscored the critical role of exact hydrological predictions for well-informed choices in water resource management and highlighted the capacity of hydrological models. **Marshall et al.,** (2024) [15] investigated the performance of enhanced informed decision-making and effective watershed management models globally, helping to develop sustainable solutions amid growing environmental pressures. **Shu et al.,** (2024) [16] underscored the capability of the coupled module as a key instrument for understanding and forecasting hydrological processes, thereby supporting more effective water natural resource planning and climate resilience strategies. **Yu et al.,** (2024) [17] offered a novel systems strategy for watershed-level nutrient monitoring and contamination control approaches, accounting for both natural and anthropogenic disturbances.

2.1 Challenges

Modeling surface water dynamics using deep learning and Geographic Information System (GIS) based spatial analytics faces several general challenges. The availability and reliability of high-quality hydrological and spatial data limit the performance of the model. Uncertainties related to climate change, land-use modifications, and human interventions further complicate accurate predictions. Overall, these challenges highlight the need for better data, efficient computational methods, and user-friendly integration for effective hydrological assessment.

2.2 Contribution

The contribution of this research lies in integrating advanced deep learning through the hybrid network with GIS-based spatial analytics to improve the accuracy and reliability of surface water dynamics modeling. By combining data-driven modeling with spatial insights, it enhances the prediction of runoff and baseflow in complex hydrological settings. This approach not only advances methodological innovation in hydrological assessment but also supports practical applications in watershed management, flood control, and ecosystem conservation.

2.3 Objectives

The research objectives of the work are:

- To delineate and characterize the sub-watersheds of Pulicat Lake using GIS and remote sensing techniques, focusing on topography and land use.
- To simulate and separate baseflow and surface runoff of Sullurpeta and Dugarajupatnam watersheds using recursive digital filter techniques.
- To integrate time-series meteorological inputs and static watershed parameters into the SWAT model for accurate hydrologic modelling.
- To examine spatial and temporal alterations in hydrological response across the sub-basins, identifying the key factors influencing runoff generation and groundwater recharge in the Pulicat Lake region.
- To develop an integrated framework combining CoatNet with GIS-based spatial analytics for accurate modeling of surface water dynamics and to improve hydrological assessment and decision-making in the Pulicat lake watershed.

3. METHODOLOGY

A comprehensive framework for hydrological assessment of Pulicat lake using GIS and remote sensing is displayed in Figure 1. The process begins with delineating and characterizing the sub-watersheds, followed by separating baseflow and surface flow components using digital filter techniques and long-term daily flow data. Time-series meteorological inputs and static watershed parameters are then integrated into the SWAT model for accurate hydrologic simulation. This is followed by the estimation of runoff generation, groundwater recharge, and analyzing spatial and temporal variations in hydrological responses across sub-basins. Finally, an integrated framework combining a hybrid convolutional–transformer network with GIS ensures accurate modeling and assessment of the watershed system.

3.1 Research Area

Pulicat Lake is located along the boundary between Andhra Pradesh and Tamil Nadu, along the southeastern coast of India, as displayed in Figure 2. It is the second-largest transitional water body in India, measuring 759 square kilometers. The present research used two watersheds, as defined by the locations of two hydrological observation stations near Sullurpeta (13º25′12.3″ N, 80º01′45.8″ E) and Dugarajupatnam (13º36′23.4″ N, 80º10′12.5″ E), which in this publication are depicted as the Sullurpeta watershed and Dugarajupatnam watershed, respectively.

The Sullurpeta watershed and Dugarajupatnam watershed are located in the northern and central part of the Pulicat lake basin, which is located in the coastal plains of

southern Andhra Pradesh and north Tamil Nadu along the eastern coast of India.

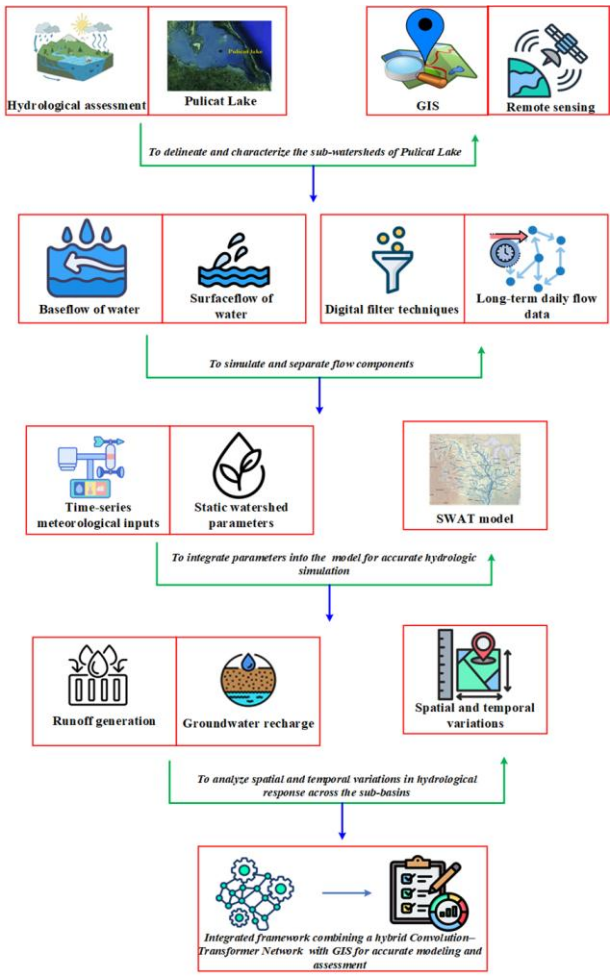

Figure 1: Framework for hydrological assessment of Pulicat lake

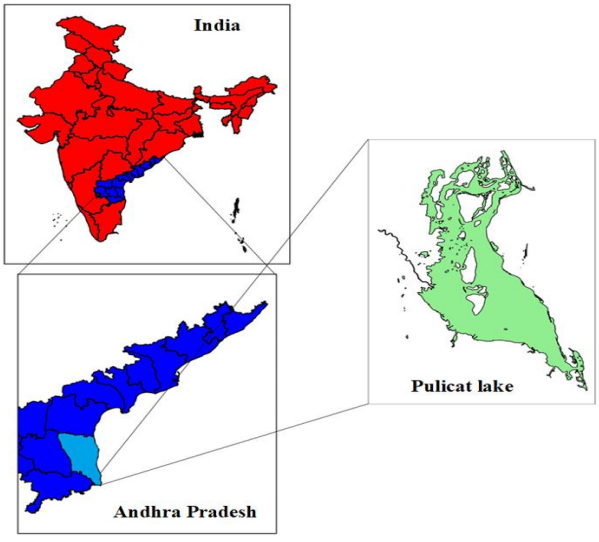

Figure 2: Location view of Pulicat lake

Table 1: Climatic records of Pulicat lake

Parameter	Sullurpeta watershed	Dugarajupatnam watershed	Data source	Remarks
Latitude	13°25′12.3″ N	13°36′23.4″ N	Field coordinates / Satellite data	Global positioning system verified coordinates
Longitude	80°01′45.8″ E	80°10′12.5″ E	Field coordinates / Satellite data	Global positioning system -verified coordinates
Mean annual rainfall (mm)	1100–1300	1050–1250	IMD (Nellore, Sullurpeta, Ponneri)	Mostly from Northeast monsoon (Oct–Dec)
Mean max temperature (°C)	32.5	33.0	IMD station data	Hottest months: May–June
Mean Min temperature (°C)	22.5	23.0	IMD station data	Coldest months: December–January
Climate type	Tropical Wet and Dry (Aw)	Tropical Wet and Dry (Aw)	Köppen climate classification	Dominated by monsoon cycles
Predominant wind direction	East to Northeast	East to Northeast	IMD climatological normals	Influences local evaporation and moisture movement
Relative humidity (%)	60–85	65–88	IMD station data	Higher during monsoon season
Evapotranspiration rate (mm/day)	4.0–5.5	4.2–5.8	FAO Penman-Monteith / field instruments	Varies with season and vegetation
Number of rainy days/years	65–85	60–80	IMD daily rainfall records	Concentrated during monsoon seasons

3.2 Data Collection

Time-series and static input data are employed for simulating the baseflow and surface runoff in the research area. The time-series data comprised daily precipitation (mm), maximum and minimum temperature (°C), and curve number for each sub-basin. Static data included sub-basin area (km^2) and the distance from each sub-basin to the lake outlet (km). The three meteorological datasets and flow records span the period from 2001 to 2019. Daily precipitation and temperature data are collected from the India Meteorological Department (IMD) stations located at Nellore, Sullurpeta, and Ponneri [Station IDs: IMD-NLR01, IMD-SLP02, and IMD-PON03]. Detailed climate information of Pulicat lake from 2001 to 2019 is provided in Table 1.

3.3 Recursive Digital Filter Technique

For Pulicat Lake, the recursive digital filter technique is applied to isolate baseflow and surface runoff from observed streamflow data, enabling a clearer

understanding of the lake's hydrological response and balance.

The component of streamflow coming from groundwater (bf) is given as,

$$bf = \frac{(1-b_{Max})\alpha b_{t=1} + (1-\alpha)b_{Max}A_t}{1-\alpha b_{Max}} \quad (1)$$

Where, t is the time, A is the total stream flow, α is the constant determinant, $b_{\max}$ is the total base flow.

3.4 Soil and Water Assessment Tool

The SWAT model is a highly versatile model capable of simulating nearly all aspects of watershed processes [18,19]. It is widely used to predict watershed responses to potential changes such as land use modifications, climate shifts, and sedimentation. The accuracy and reliability of its simulations heavily rely on the integrity of the input data used during model setup.

$$SM_F = SM_I + \sum_{i=1}^{x}(P - S - E - W - RF) \quad (2)$$

where, SM_F and SM_I is the final daily moisture content of the soil, P is the daily amount of precipitation, S is the daily surface runoff, E is the daily evaporation, W is the amount of daily entering water, and RF is the daily return flow at time x.

The retention parameter (R_p) is given as,

$$R_p = 25.4\left(\frac{100}{Cr_{No}} - 10\right) \quad (3)$$

where, Cr_{No} is the curve number of the day.
Nash–Sutcliffe Efficiency (nse) is defined as,

$$nse = 1 - \frac{\sum_{i=0}^{q}(P_{o,i} - P_s)^2}{\sum_{i=0}^{q}(P_{o,i} - P_o)^2} \quad (4)$$

The root mean square error (RME) is given as,

$$RME = \frac{\sqrt{\sum_{i=0}^{q}\left(P_o - P_s\right)_i^2}}{\sqrt{\sum_{i=0}^{q}\left(P_o - \overline{P_s}\right)^2}} \quad (5)$$

where, P_o and P_s are the observed and simulated hydrological variables in the location i, and q is the number of observations.

3.5 Hybrid Convolution–Transformer Network

A CoatNet model is trained to predict the spatial analytics of Pulicat lake under research. Python 3.11.4 and Google Colab, employing key libraries such as OpenCV, Pillow, TensorFlow, Keras, Matplotlib, Seaborn, Detectron2, fastai, are used for designing the hybrid Coat Net module. Data augmentation is accomplished by horizontal flipping, resulting in 125 images, used to train and optimize the configuration. Each image is used as an input with associated variables employed as identifiers. The generated outcomes are filtered, and the process is displayed in Figure 3.

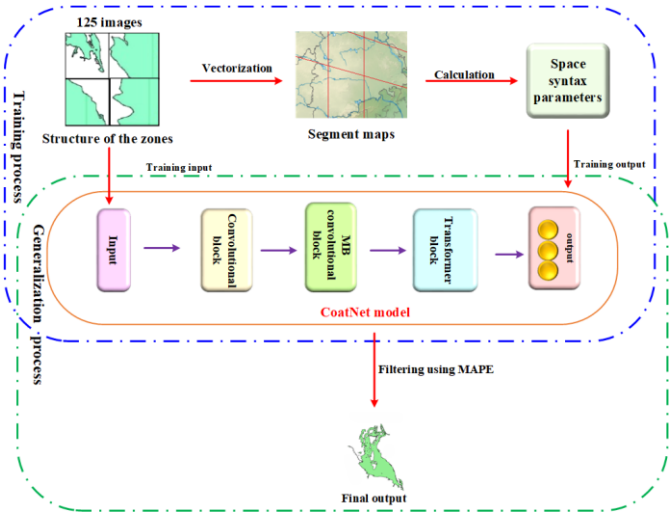

Figure 3: Overview of the generation and optimisation process

3.6 Spatial Analytics

The basic theoretical framework of space analytics emerges from the concepts of connectivity and accessibility in topology [20,21]. The ratio between the theoretically maximum generalized distance (ITi) is given as,

$$ITi = a^2 / \sum_{i=1}^{a} D(j,i),\ j \neq i \quad (6)$$

where, a is the total number of nodes, D is the distance from the segment j to the other segment i.

In the assessment stage, Mean Absolute Percentage Error (MAPE) is introduced, including the coefficient of determination (R^2). MAPE is expressed as,

$$MAPE = \frac{100\%}{X}\sum_{i=1}^{X}\left|\frac{\hat{z}_i - z_i}{z_i}\right| \quad (7)$$

where, z_i is the actual value, $\hat{z}_i$ is the predicted value, and the absolute value of the components is summed and divided by the total number X .

4. RESULT AND DISCUSSION

The hydrological behavior of the Pulicat lake by integrating GIS-based watershed characterization, SWAT model simulations, and advanced deep learning approaches is discussed in the section below. These evaluations facilitate a broad understanding of the hydrological response of the Pulicat lake region, supporting better assessment and sustainable watershed management.

4.1 Topographic Analysis

The slope and orientation of Pulicat lake based on GIS and remote sensing are displayed in Figure 4. The regions with low slope are displayed in lemon yellow colour, and steeper regions are represented in pale green colour. The lake is slightly flat, as illustrated by the orange colour, and the bright yellow colour represents the low slope regions. Henceforth, the lake is slightly flat with gently sloping regions.

The slope direction of Pulicat lake based on GIS and remote sensing is displayed in Figure. The largest area in the research area is located in the West and possesses smaller flat areas. The slopes are classified according to the geographical directions and the interaction of the terrain with the natural factors.

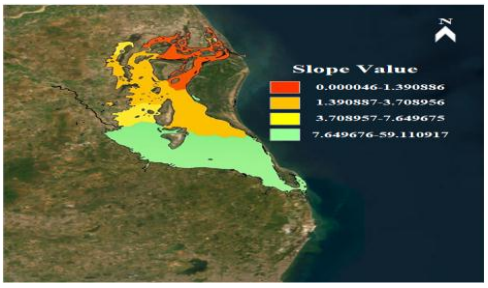

Figure 4: Slope and orientation of Pulicat lake

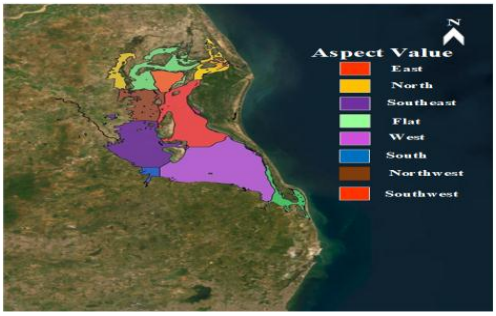

Figure 5: Slope direction of Pulicat lake

The land use around Pulicat lake is characterised by four major categories, as displayed in Figure 6. The forest area dominates the region, covering most of the surroundings of the lake. The built-up areas are concentrated mainly in the northern part, reflecting human settlements and infrastructure near the lake. Cultivated lands appear in patches, especially along the southern and southeastern parts, indicating agricultural activity. A highway runs across the southern side of the lake, providing connectivity but also influencing land use dynamics. Overall, the map highlights a mix of natural and human-modified landscapes, with forest cover as the most prominent feature.

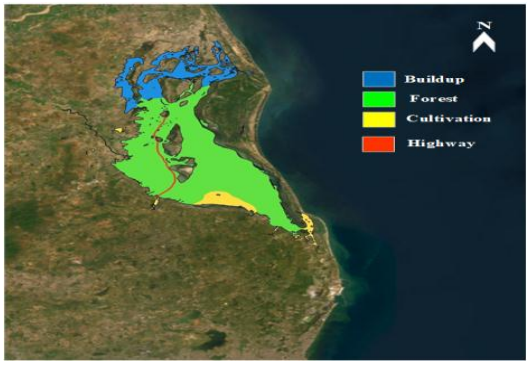

Figure 6: land use around Pulicat lake

4.2 Baseflow and Surface Runoff of Watersheds

The baseflow and surface runoff of the Sullurpeta watershed during 2001 to 2019 are displayed in Figure 7. The baseflow generally dominates the hydrological contribution, ranging mostly between 8,000 and 20,000 m^3/day during 2001–2010. The maximum base flow of the Sullurpeta watershed ranged around 70,000 m^3/day during 2017. The Surface runoff is lower but follows a similar trend, fluctuating between 5,000 and 12,000 m^3/day in the early years, with notable increases up to 30,000–35,000 m^3/day during high-flow years such as 2012 and 2017.

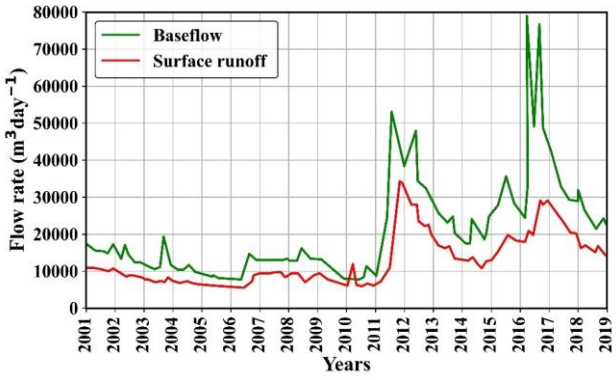

Figure 7: Baseflow and surface runoff of the Sullurpeta watershed

The baseflow and surface runoff of the Dugarajupatnam watershed during 2001 to 2019 are displayed in Figure 8. The observations suggested that baseflow contributes a larger share of streamflow compared to surface runoff, with both components reflecting rainfall variability, and extreme events driving significant peaks in 2012 and 2017. The baseflow and surface flow of Dugarajupatnam watershed are maximum with 60,000 m^3/day in 2016–2017 and 30,000–35,000 m^3/day during 2017, respectively.

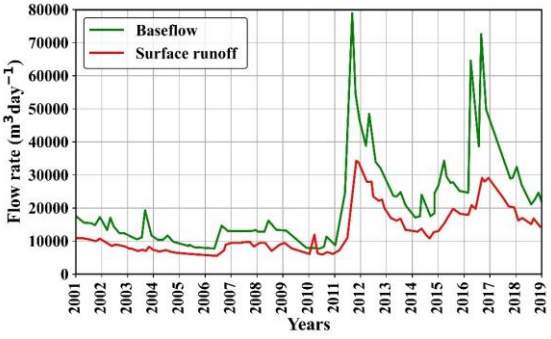

Figure 8: Baseflow and surface runoff of the Dugarajupatnam watershed

4.3 Sensitivity Analysis of the Hydrological Modeling Tool

To enhance the reliability of the model, a sensitivity analysis is performed on five key parameters, representing the hydrological process in the Pulicat lake is presented in Table 2. These parameters include precipitation, temperature, area, curve number, and distance to outlet.

Table 2: Parameters included in sensitivity analysis

Parameter	Description
RCN_PCP	Precipitation
RCN_TMP	Temperature
HRU_FR	Area
C_N2	Curve number
DRU_SLP	Distance to outlet

The outcomes of the sensitivity analysis indicated that out of five parameters, three are statistically significant, as displayed in Figure 9. The p and t validations are significant for
precipitation ($p = 0.01, \mathrm{t} = -10.0$),
temperature ($p = 0.02, \mathrm{t} = -15.0$),
and curve number ($p = 0.03, \mathrm{t} = -8.0$), and showed low p-value ($\prec 0.05$) and strong t-statistics ($\succ 2$).

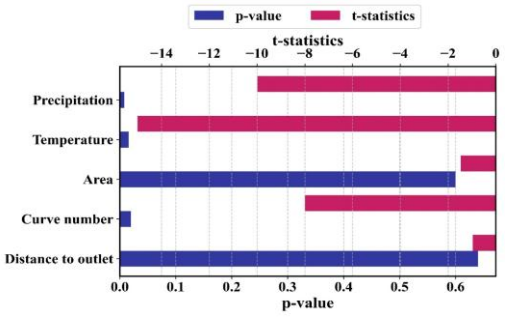

Figure 9: Outcomes of the sensitivity analysis

The dot plot for precipitation is displayed in Figure 10, representing the dispersion of precipitation against the corresponding *nse* values. The clear trend in the data plots indicated the sensitivity of the parameter influencing *nse* values. This sensitivity emphasizes the critical role of precipitation in driving surface runoff, streamflow generation, and overall watershed response, thereby underlining its importance in accurate model simulation and performance assessment.

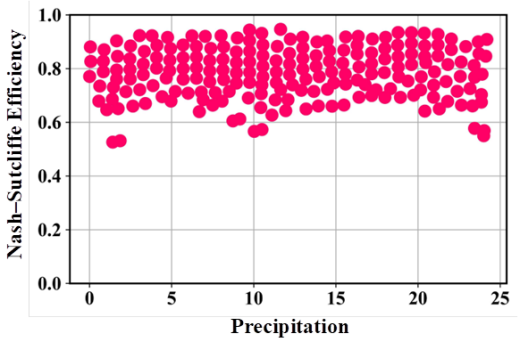

Figure 10: Distribution of precipitation

The dot plot across temperature is displayed in Figure 11, and the dense clustering of the data indicates the sensitivity of temperature. The data plots of temperature are clustered around 0.6 and 0.9 *nse* values. The observed sensitivity highlights the importance of considering temperature variability in modeling to ensure reliable predictions under changing climate conditions.

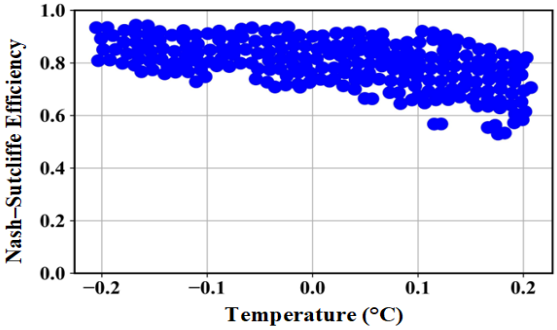

Figure 11: Distribution of Temperature

The dot plot displayed in Figure 12 for the parameter fractional area increases, and the performance of the model is consistently high, with 0.82 *nse*. The lower points are around 0.55 to 0.6 *nse* degrade the performance, but overall, the model for the parameter fractional area is robust and stable. This stability underscores the resilience of the model in handling spatial distribution parameters for the Pulicat lake ecosystem.

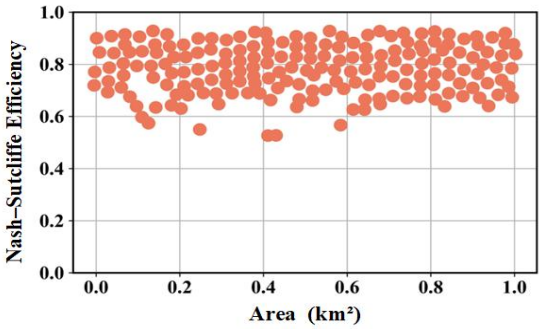

Figure 12: Distribution of area

The performance of the model is strong for the parameter curve number as displayed in Figure 13. The mean performance across all values appears to be around 0.82 to 0.85 *nse*, with a few low outliers near 0.55 to 0.6 *nse*. The accurate calibration of this parameter is essential for capturing the rainfall–runoff relationship over the Pulicat lake region.

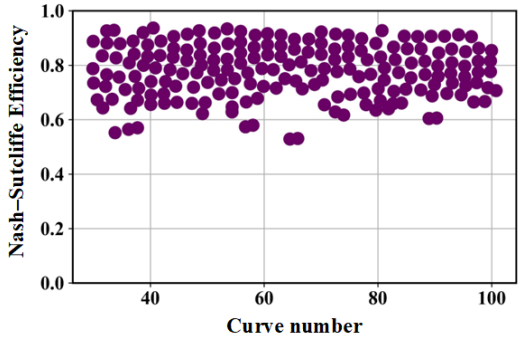

Figure 13: Distribution of curve number

The average value of *nse* is about 0.85, indicating stable calibration results for the parameter distance to outlet as displayed in Figure 14. The observed stability confirms that the model effectively captures watershed-scale routing processes, supporting its applicability for long-term hydrological assessment and management of the Pulicat lake system.

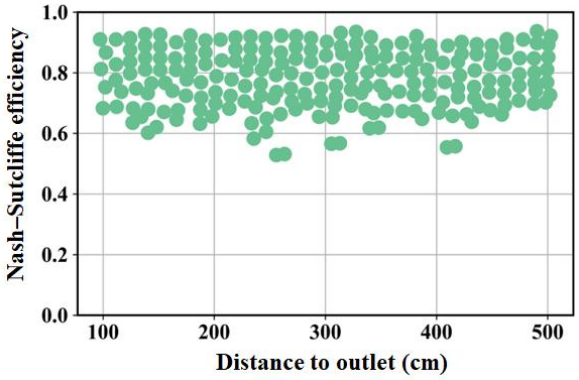

Figure 14: Distribution of distance to outlet

Based on the results above, three parameters are chosen for calibrating the model, and the final calibrated parameters are shown in Table 3. The fitted values fall within the calibration range, indicating that the model remains stable.

Table 3: Selected parameters, with their best fitted values

Parameter	Fitted Validation	Minimum	Maximum
RCN_PCP	0.0500	−0.20	0.20
RCN_TMP	− 0.0300	−0.20	0.20
C_N2	-0.0604	−0.20	0.20

4.3.1 Performance of Hydrological Modelling Tool

During the calibration period of 2001 to 2009, the model attained an *nse* of 0.96, suggesting 96 % of variance. The value of R^2 is 0.94, illustrating a significant linear correlation between the predicted and actual data as displayed in Figure 15.

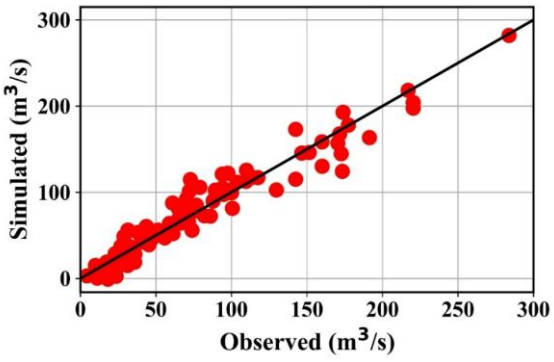

Figure 15: Predicted and actual data streamflow for calibration phase

The *nse* and R^2 value for the validation period of 2010 to 2019 is 0.92 and 0.90, respectively, illustrating the high level predictive capability of the model. The monitored data for the validation period are displayed in Figure 16, and the accuracy of the SWAT model is presented in Table 4.

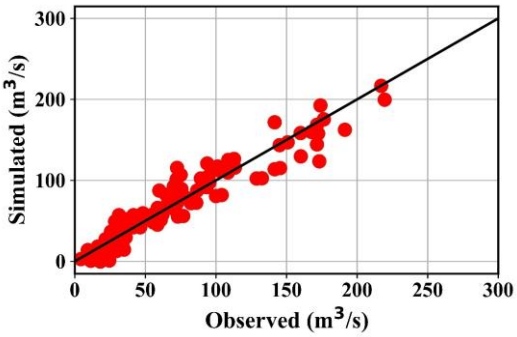

Figure 16: Predicted and actual data streamflow for validation phase

The calibration and validation results showcase reliable model results, with calibration values of 0.94 and 0.96 and corresponding validation values of 0.90 and 0.92, showing strong agreement between predicted and actual data during both phases. The error values of calibration and validation are 0.22 and 0.31, respectively, illustrating the consistency and resilience of the model. Overall, the results demonstrate good model efficiency and generalization capability.

Table 4: SWAT performance accuracy during calibration and validation at Pulicat lake

Metric	Calibration	Validation
R^2	0.94	0.90
nse	0.96	0.92
RME	0.22	0.31

The observed and simulated streamflow at Pulicat lake is displayed in Figure 17, and the precalibrated model satisfactorily replicated the seasonal flow regime ranging from about 50 to 450 m^3/s. High flows appear during the monsoon when rainfall goes above 400 to 500 mm, while in dry months the flow drops below 100 m^3/s.

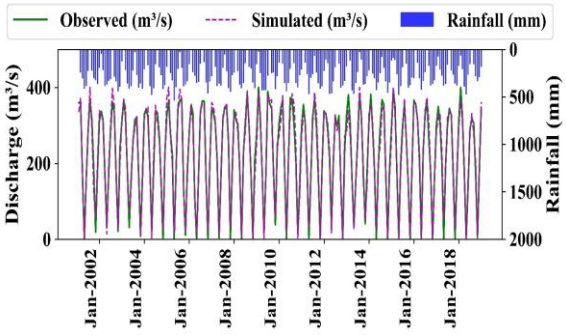

Figure 17: Observed and simulated streamflow at Pulicat lake before calibration

The observed and simulated streamflow at Pulicat lake, along with rainfall after calibration, is displayed in Figure 18. The simulation outcomes are improved, and the seasonal variations driven by rainfall events are captured well. The overlap between observed and simulated lines indicates that the calibration process significantly improved the accuracy of the model in reproducing the hydrological behavior of Pulicat lake.

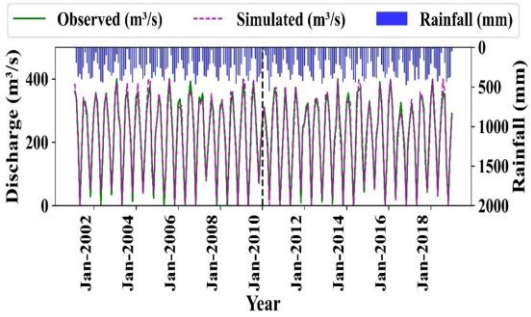

Figure 18: Observed and simulated streamflow at Pulicat lake after calibration

4.4 Spatial and Temporal Variation in Surface Runoff

The spatial variation of surface runoff in Pulicat lake and its simulated outcome with significant spatial variation is displayed in Figure 19. The lowest runoff is observed over the northern part of the basin, with less than 15 mm surface runoff, and the southeast experiences very high runoff exceeding 60 mm. The central and southern zones exhibit moderate runoff between 15–45 mm. This spatial distribution highlighted the contribution of topography, land use, and rainfall intensity on surface runoff patterns within the Pulicat lake.

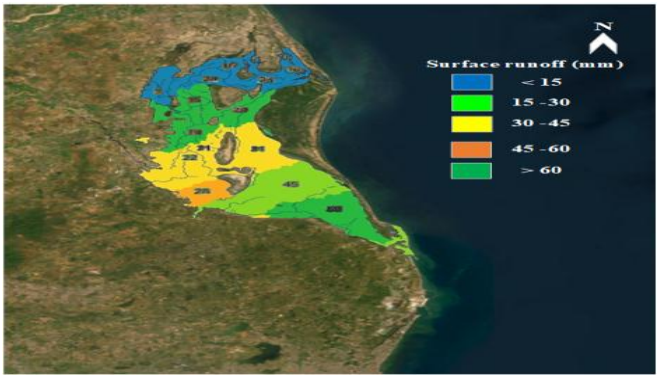

Figure 19: Spatial variation of surface runoff in Pulicat lake

The average annual surface runoff in Pulicat lake from 2001 to 2019 is displayed in Figure 20. The runoff is highest in 2001, 2006, and 2013, each reaching close to 60 mm, while the lowest values are recorded in 2015 and 2017 at around

21 to 22 mm. 2004, 2015, and 2017 recorded the lowest surface runoff.

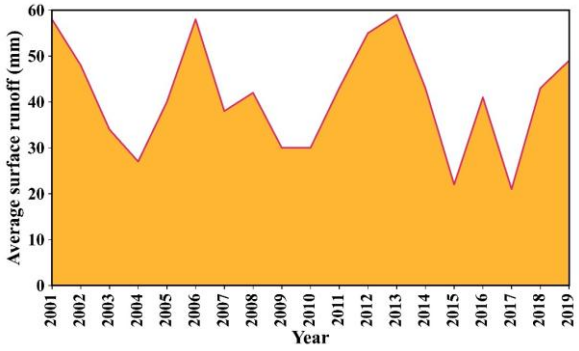

Figure 20: Average annual surface runoff in Pulicat lake from 2001 to 2019

The monthly average surface runoff in Pulicat lake from 2001 to 2019 is displayed in the Figure 21. The observations reflected the influence of seasonal rainfall variations, particularly during the monsoon months. 2003, 2010, and 2018 indicated runoff below 50 mm, while 2001, 2004, 2006, 2010, and 2015 approached 200 mm, with the highest runoff. Overall, the data highlights the seasonal and interannual variability of hydrological response in the Pulicat lake region, with fluctuations in runoff driven largely by rainfall intensity and distribution.

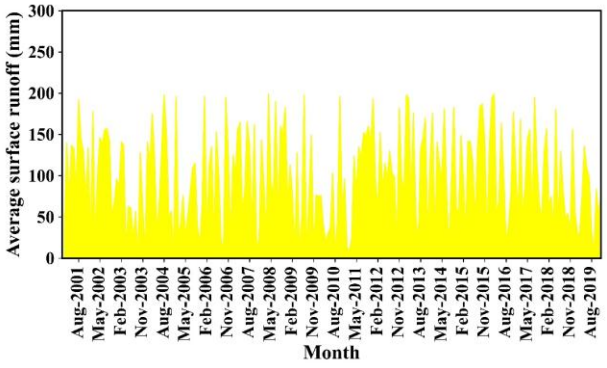

Figure 21: Monthly average surface runoff in Pulicat lake from 2001 to 2019

4.5 Spatial and Temporal Variation in Groundwater Recharge

The spatial variation of groundwater recharge in the Pulicat lake watershed shows a distinct north–south pattern as displayed in Figure 22. The northern and central regions predominantly experienced moderate recharge levels, ranging from 30 to 45 mm. Some localized zones in the upper basin showed higher recharge, between 45 to 60 mm. In contrast, the southern and southeastern parts of the watershed record comparatively low recharge values below 15 mm and 15 to 30 mm. Overall, the distribution indicates that groundwater recharge is more favorable in the central portions, while peripheral areas, particularly in the south, observed relatively low recharge potential.

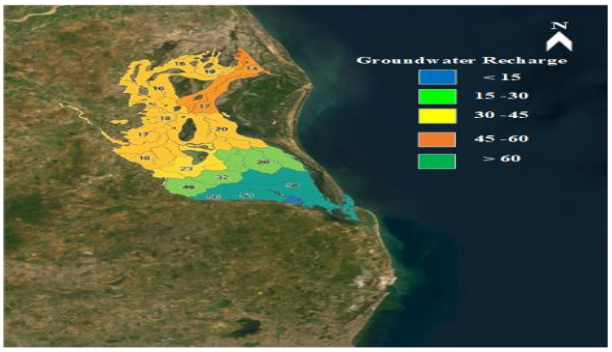

Figure 22: Spatial variation of groundwater recharge in the Pulicat lake

The average annual groundwater recharge in Pulicat lake varied from 2001 to 2019, as displayed in Figure 23. Years such as 2001,2006, and 2013 recorded higher recharge, while 2004, 2007, 2009, 2010, 2015, and 2017 featured the lowest groundwater recharge. The variation in groundwater recharge in Pulicat lake between 2001 and 2019 is mainly due to changes in rainfall patterns. In addition, factors like the usage of land, over-extraction of groundwater, and reduced wetland area contributed to the decline in recharge in certain years.

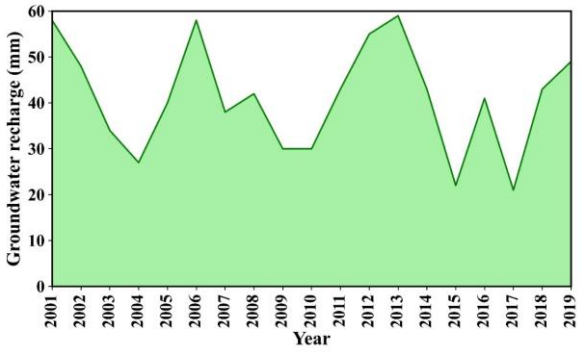

Figure 23: Annual groundwater recharge in Pulicat lake varied from 2001 to 2019

The monthly average groundwater recharge of Pulicat lake is displayed in Figure 24. The groundwater recharge is minimal during the dry seasons of November to March and maximum during the wet seasons of June to August. Moreover, 2003 and 2009 exhibited the lowest groundwater recharge across the months.

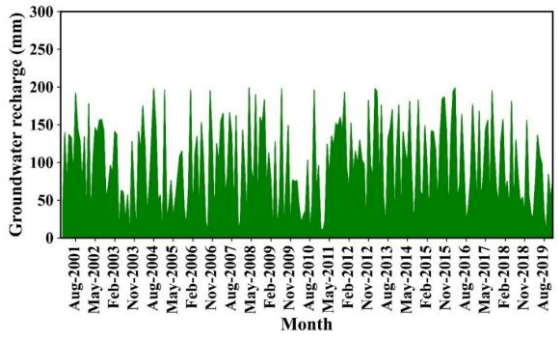

Figure 24: Monthly average groundwater recharge of Pulicat lake

4.6 Spatial Analytics of Pulicat Lake by Hybrid Convolution–Transformer Network

The hydrological integration across the entire watershed of Pulicat lake is described as INT PL, and the local integration INT 1000 m represents the connectivity of wetlands, channels, or marshes within a localized area. The critical hydrological assessment based on the corridors is described as Choice PL and Choice 1000 m are the smaller hydrological connections that locally dominate the movement of water in Pulicat lake. The river lines for the selected zones of Pulicat lake for analysis are displayed in Figure 25.

Figure 25: River lines for the selected zones of Pulicat lake

The average values of spatial analytics parameters such as INT PL, INT 1000 m, Choice PL, and Choice 1000 m in terms of the hydrological context for real samples are presented in Table 5. The east zone possesses the highest global and local integration, making the east zone the central node for connectivity and flow. The North zone has the lowest integration and choice values, showing that it is the least connected, thereby highlighting the supporting role of the West and South zones.

Table 5: Mean values of space syntax parameters

Zone	INT PL	INT 1000 m	Choice PL	Choice 1000 m
East	480.3	105.6	3,100.5	132.4
West	420.7	88.2	2,450.7	108.7
North	365.4	72.4	1,900.2	76.3
South	390.1	80.3	2,050.9	82.9

4.6.1 Training

After data amplification, 200 training samples are used for training, and 125 samples are used as a validation set. After adjusting the parameter and iteration, the MAPE on the training and validation set reaches 10.34 % and 12.13 % respectively, after 78 epochs. After screening, a MAPE of 12.13 % is achieved as displayed in Figure 26.

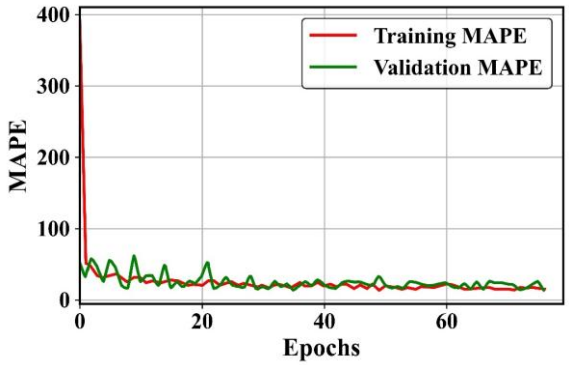

Figure 26: MAPE of training and validation set

4.6.2 Testing

The predicted MAPE for the spatial analytics parameters in terms of the hydrological context is presented in Table 6. The error in predicting global integration is relatively low, and global choice has the highest error of 17.95 %. On average, the model has about a 15% error rate, which is considered acceptable in spatial and hydrological modeling, showing that the framework produces reliable results.

Table 6: MAPE for the spatial analytics parameters

Parameters	MAPE (%)
INT PL	12.37
INT 1000 m	15.42
Choice PL	17.95
Choice 1000 m	13.11
Average	14.71

5. CONCLUSION AND FUTURE SCOPE

The present research is undertaken to perform the hydrological modeling of Pulicat lake with Sullurpeta and Dugarajupatnam watershed. The slope and orientation of Pulicat lake based on GIS and remote sensing, revealed that the lake is slightly flat with gently sloping regions. The land use analysis highlighted a mix of natural and human-modified landscapes, with forest cover the most prominent feature. The baseflow and surface runoff of the Sullurpeta and Dugarajupatnam watershed during 2001 to 2019 are simulated using recursive digital filter techniques. To reduce the uncertainty of the model, a sensitivity analysis is performed on five SWAT key parameters. The p and t validations are significant for precipitation ($p = 0.01, \mathrm{t} = -10.0$), temperature ($p = 0.02, \mathrm{t} = -15.0$), and curve number ($p = 0.03, \mathrm{t} = -8.0$), displaying low p-value and strong t-statistics. During the calibration period of 2001 to 2009, the model achieved an nse of 0.96, suggesting 96 % of variance. The nse and R^2 value for the validation period of 2010 to 2019 is 0.92 and 0.90, respectively, illustrating the high level performance of the model. The observed and simulated streamflow at Pulicat lake, along with rainfall explored that the calibration process significantly advanced the accuracy of the model in reproducing the hydrological behavior of Pulicat lake. The spatial and temporal variations in surface runoff and groundwater recharge are also captured. In addition, the incorporation of a hybrid CoatNet deep learning framework with GIS-based spatial analytics enhanced the accuracy of modeling surface water dynamics. On average, the model has about a 15% error rate, which is considered acceptable in spatial and hydrological modeling, showing that the framework produces reliable results.

The future scope of this study lies in extending the hybrid CoatNet–GIS framework to larger and more diverse watersheds for improved scalability and adaptability. It can also be integrated with climate change projections and real-time data to enhance predictive hydrological assessments and support proactive water resource management.

REFERENCES

[1] Nan, T., Cao, W., Wang, Z., Gao, Y., Zhao, L., Sun, X. and Na, J., 2023. Evaluation of shallow groundwater dynamics after water supplement in North China Plain based on attention-GRU model. Journal of Hydrology, 625, p.130085.

[2] Abeshu, G.W., Tian, F., Wild, T., Zhao, M., Turner, S., Chowdhury, A.K., Vernon, C.R., Hu, H., Zhuang, Y., Hejazi, M. and Li, H.Y., 2023. Enhancing the representation of water management in global hydrological models. Geoscientific Model Development, 16(18), pp.5449-5472.

[3] Yao, J., Xu, N., Wang, M., Liu, T., Lu, H., Cao, Y., Tang, X., Mo, F., Chang, H., Gong, H. and Xin, H., 2025. SWOT satellite for global hydrological applications: Accuracy assessment and insights into surface water dynamics. International Journal of Digital Earth, 18(1), p.2472924.

[4] Abbas, S.A., Bailey, R.T., White, J.T., Arnold, J.G. and White, M.J., 2024. Quantifying the Role of Calibration Strategies on Surface-Subsurface Hydrologic Model Performance. Hydrological Processes, 38(10), p.e15298.

[5] Yao, J., Xu, N., Wang, M., Gong, P., Lu, H., Cao, Y., Tang, X. and Mo, F., 2024. Promoting global surface water monitoring research with the SWOT satellite. The Innovation Geoscience, 2(4), pp.100099-100100.

[6] Petpongpan, C., Ekkawatpanit, C., H. Gheewala, S., Visessri, S., Saraphirom, P., Kositgittiwong, D. and Kazama, S., 2025. Integrated management of surface water and groundwater for climate change adaptation using hydrological modeling. Environment, Development and Sustainability, 27(6), pp.14321-14341.

[7] Yohannes, H., Argaw, M. and Seifu, W., 2024. Impact of land use/land cover change on surface water hydrology in Akaki river catchment, Awash basin, Ethiopia. Physics and Chemistry of the Earth, Parts A/B/C, 135, p.103690.

[8] Wang, X., Liu, Z., Xu, Y.J., Mao, B., Jia, S., Wang, C., Ji, X. and Lv, Q., 2025. Revealing nitrate sources seasonal difference between groundwater and surface water in China's largest fresh water lake (Poyang Lake): Insights from sources proportion, dynamic evolution and driving forces. Science of The Total Environment, 958, p.178134.

[9] Wang, F., Liu, L., Xu, H., Liu, Y., Meng, X. and Peng, B., 2025. An analytical solution model of oil–water dynamic imbibition considering dynamic contact angle effect and osmotic pressure at micro-nano scale. Fuel, 379, p.132979.

[10] Lyu, K., Dong, Y., Lyu, W., Zhou, Y., Wang, S., Wang, Z., Cui, W., Zhang, Y., Zhang, Q. and Cui, Y., 2025. Data-driven and numerical simulation coupling to quantify the impact of ecological water replenishment on surface water-groundwater interactions. Journal of Hydrology, 649, p.132508.

[11] Bojer, A.K., Abshare, M.W., Mesfin, F. and Al-Quraishi, A.M.F., 2025. Assessing climate and land use impacts on surface water yield using remote sensing and machine learning. Scientific Reports, 15(1), p.18477.

[12] Shiferaw, N., Habte, L. and Waleed, M., 2025. Land use dynamics and their impact on hydrology and water quality of a river catchment: a comprehensive analysis and future scenario. Environmental Science and Pollution Research, 32(7), pp.4124-4136.

[13] Liu, C.Y., Huang, P.Y., Hsu, S.Y., Tung, C.P. and Liao, K.W., 2025. Anthropogenic drought monitoring using socio-hydrological modeling for surface water deficit: Lessons from Northern Taiwan. Journal of Hydrology, 647, p.132298.

[14] Kumar, M., Tiwari, R.K., Rautela, K.S., Kumar, K., Khajuria, V., Verma, I., Safi, S., Almazroui, M., Al Kafy, A.,

Zhang, L. and Elhag, M., 2025. Comparative assessment of process based models for simulating the hydrological response of the Himalayan River Basin. Earth Systems and Environment, 9(1), pp.299-313.

[15] Marshall, S.R., Tran, T.N.D., Tapas, M.R. and Nguyen, B.Q., 2025. Integrating artificial intelligence and machine learning in hydrological modeling for sustainable resource management. International Journal of River Basin Management, pp.1-17.

[16] Shu, L., Li, X., Chang, Y., Meng, X., Chen, H., Qi, Y., Wang, H., Li, Z. and Lyu, S., 2024. Advancing understanding of lake–watershed hydrology: a fully coupled numerical model illustrated by Qinghai Lake. Hydrology and Earth System Sciences, 28(7), pp.1477-1491.

[17] Yu, J., Tian, Y., Wang, X., Sun, T., Lancia, M., Andrews, C.B. and Zheng, C., 2024. Integrated modeling of flow, soil erosion, and nutrient dynamics in a regional watershed: Assessing natural and human-induced impacts. Water Resources Research, 60(9), p.e2024WR037531.

[18] Lee, J., Han, J., Engel, B. and Lim, K.J., 2025. Web-Based Baseflow Estimation in SWAT Considering Spatiotemporal Recession Characteristics Using Machine Learning. Environments, 12(3), p.94.

[19] Mei, Z., Peng, T., Chen, L., Singh, V.P., Yi, B., Leng, Z., Gan, X. and Xie, T., 2025. Coupling SWAT and LSTM for improving daily streamflow simulation in a humid and semi-humid river basin. Water Resources Management, 39(1), pp.397-418.

[20] Radman, A., Mohammadimanesh, F. and Mahdianpari, M., 2024. Wet-ConViT: A Hybrid Convolutional–Transformer Model for Efficient Wetland Classification Using Satellite Data. Remote Sensing, 16(14), p.2673.

[21] Fahim-Ul-Islam, M., Chakrabarty, A., Ahmed, S.T., Rahman, R., Kwon, H.H. and Piran, M.J., 2024. A comprehensive approach towards wheat leaf disease identification leveraging transformer models and federated learning. IEEE Access.